MOLECULAR AND CELLULAR BIOLOGY, Dec. 2005, p. 10768–10781 Vol. 25, No. 24
0270-7306/05/$08.00+0 doi:10.1128/MCB.25.24.10768–10781.2005

Involvement of Prep1 in the αβ T-Cell Receptor T-Lymphocytic Potential of Hematopoietic Precursors

Dmitri Penkov,[1,2]† Patrizia Di Rosa,[1,2] Luis Fernandez Diaz,[1,2] Veronica Basso,[3] Elisabetta Ferretti,[1,2]‡ Fabio Grassi,[4] Anna Mondino,[3] and Francesco Blasi[1,2]*

Molecular Genetics Unit, Università Vita Salute San Raffaele, via Olgettina 58, 20132 Milan, Italy[1]*; IFOM (FIRC Institute of Molecular Oncology), via Adamello 14, 20016 Milan, Italy*[2]*; Lymphocyte Activation Unit, Istituto Scientifico San Raffaele, Milan, Italy*[3]*; and Institute of Research in Biomedicine, V. V. Vela, Bellinzona, Switzerland*[4]

Received 13 July 2005/Returned for modification 28 August 2005/Accepted 23 September 2005

Prep1 is a homeodomain transcription factor that acts by dimerizing with Pbx. Since *Prep1* null embryos die at gastrulation, we studied *Prep1*$^{i/i}$ hypomorphic mice to study the physiological role of *Prep1*. A low percentage of homozygous *Prep1*$^{i/i}$ mice survived at birth, and their postnatal functions could be investigated. Reduced *Prep1* expression caused an abnormal thymic T-cell development: increased CD4$^-$ CD8$^-$ double-negative thymocytes, decrease in αβTCR^{high} cells (cells with high levels of the αβT-cell receptor [αβTCR]) and CD4$^+$ and CD8$^+$ single-positive (SP) thymocytes, and increase in γδTCR cells. Peripheral lymphoid organs of *Prep1*$^{i/i}$ mice contained fewer αβTCR mature T cells and more γδTCR T cells than wild-type littermates. Moreover, *Prep1*$^{i/i}$ CD4$^+$ CD8$^+$ double-positive thymocytes underwent more apoptosis, and SP thymocytes proliferated less than control littermates. Mice that were lethally irradiated and then had *Prep1*$^{i/i}$ fetal liver cells transplanted showed the same defects as the *Prep1*$^{i/i}$ mice did. Among PBC family members, Pbx2 and very low levels of Pbx3 were observed in the thymi of wild-type mice. In *Prep1*$^{i/i}$ mice, the level of Pbx2 protein was profoundly decreased, while for Pbx3 no definitive conclusion could be reached. Therefore, the deficient postnatal T-lymphocytic potential of the *Prep1* hematopoietic progenitors depends on the combined, not compensated, absence of Prep1 and at least Pbx2.

Prep1 is a transcription factor belonging to the TALE (*t*hree-*a*mino-acid *l*oop *e*xtension) family, which in vertebrates is made up of homeodomain proteins belonging to the PBC (Pbx1 to Pbx4), Prep (Prep1 and Prep2), and Meis (Meis1 to Meis3) subfamilies (10, 19).

Mammalian Pbx and Prep proteins perform essential functions in development. The role of *Prep1* in development has been studied in the zebra fish and mouse. In zebra fish, *Prep1.1* down-regulation leads to an embryonic lethal phenotype, with major homeotic defects which include the loss of expression of several anterior *Hox* genes, weak circulation, and neural and cranial abnormalities (14). Prep1 is expressed ubiquitously in the embryonic and adult mouse but at different levels in different organs (18). A *Prep1* null mutation causes lethality around gastrulation (L. C. Fernandez-Diaz, N. G. Copeland, and F. Blasi, unpublished data) while an hypomorphic mouse (*Prep1*$^{i/i}$) has a leaky embryonic lethal phenotype characterized mostly by hematopoietic and angiogenic defects (E. Ferretti, P. Di Rosa, J.-C. Villaescuss, L. C. Fernandez-Diaz, E. Longobardi, R. Mazzieri, A. Miccio, N. Micali, C. Ferrai, V. M. Diaz, L. Selleri, G. Ferrari, and F. Blasi, submitted for publication).

In mice, the ablation of the *Pbx1* gene leads to embryonic lethality around embryonic day 15.5 (E15.5), with a variety of developmental defects in head skeleton specification and differentiation (43), maintenance of definitive hematopoiesis (16), and pancreas, kidney, and thymus organogenesis (26, 42). *Pbx2*$^{-/-}$ mice are asymptomatic, while *Pbx3*$^{-/-}$ mice die at birth (P0) due to deficient central hypoventilation (39, 44).

The deletion of the mouse *Meis1* gene causes embryonic lethality and major hematopoietic defects (4, 23). Therefore, at least *Pbx1*, *Meis1*, and *Prep1* genes are involved in various aspects of hematopoiesis. However, little information is available on the roles of these proteins in T-cell development.

Prep1 and Pbx are also expressed in the adult and therefore are likely to perform important postnatal functions that are only partially known. In fact, the thymus is one of the organs in which *Prep1* expression is highest in both the embryo and adult (18). *Pbx1* and *Pbx3*, on the other hand, are expressed in hematopoietic stem cells (16, 38) but are down-regulated at the start of T-cell development, while Pbx2 is turned on at this time and is then expressed throughout (46). However, T-cell development is not affected in *Pbx2*$^{-/-}$ mice, in which the overall level of Pbx proteins is not changed, as the absence of Pbx2 is compensated for by other *Pbx* family members (44). No information is available on the expression of *Meis* genes in the thymus.

Prep1 protein is regulated by the heterodimerization with members of the Pbx and Meinox families (8–11, 19, 21). Vertebrate Prep proteins lack a nuclear localization signal and need to dimerize with Pbx to enter the nucleus, while in dimeric forms they protect Pbx from being exported from the nucleus (6, 19).

Prep and Meis proteins may also control the level of their Pbx partners. Overexpression of *Prep1* increases the half-life

* Corresponding author. Mailing address: DIBIT, Università Vita Salute San Raffaele, via Olgettina 58, 20132 Milan, Italy. Phone: 39-02-2643 4744. Fax: 39-02-2643 4844. E-mail: Blasi.Francesco@hsr.it.

† Present address: Belozersky Institute of Physico-Chemical Biology, Moscow State University, Moscow, Russia.

‡ Present address: Department of Cell and Developmental Biology, Weill Medical College, Cornell University, New York, NY 10021.

(and hence the level) of Pbx2 and Pbx1 in F9 cell lines by preventing their proteasomal degradation (30). On the other hand, down-regulation of Prep1 in zebra fish causes a drastic decrease in Pbx2 and Pbx4, and in the mouse, it causes a decrease in all Pbx proteins (15; Ferretti et al., submitted). Likewise, overexpression of *Meis1* results in an increased level of Pbx4 in zebra fish embryos by a posttranscriptional protein-stabilizing mechanism (51).

The high level of expression of *Prep1* suggests its involvement in thymus development and/or function. We have studied a hypomorphic *Prep1*$^{i/i}$ mouse line that expresses 5 to 10% of the normal level of Prep1. *Prep1*$^{i/i}$ embryos die between E17.5 and P0 and present a profound alteration in the hematopoietic development with a deficient radioprotection activity of fetal liver (FL) progenitors and all colony-forming progenitors and profound anemia (Ferretti et al., submitted). However, a small percentage of the *Prep1*$^{i/i}$ embryos are born alive and subsequently live for at least 14 months. In this study, we examined these *Prep1*$^{i/i}$ mice to study postnatal T-cell development. We explored expression of the TALE family proteins in the thymi of wild-type (wt) mice and confirmed that *Prep1* and *Pbx2* are highly expressed, *Pbx3* is expressed at low levels, but none of the other *Pbx* and *Meis* gene products were detected. *Prep1*-deficient mice displayed a complex phenotype, with a decrease in CD4$^+$ and CD8$^+$ lymphocytes, an increase in γδ T cells in the periphery, and a deficient thymocyte development in the thymus, characterized by an increase in CD4$^-$ CD8$^-$ double-negative (DN) thymocytes and γδ T-cell progenitors and a decrease in CD4$^+$ and CD8$^+$ single-positive (SP) cells. These defects were intrinsic to hematopoietic progenitors, since the T-cell phenotype of mice that survived lethal irradiation and transplantation of *Prep1*$^{i/i}$ fetal liver cells was similar to that of adult *Prep1*$^{i/i}$ mice. Importantly, in *Prep1*$^{i/i}$ cells the level of Pbx2 was essentially undetectable, indicating that both Prep1 and Pbx2 are required for proper T-cell development.

MATERIALS AND METHODS

Generation of *Prep1*$^{i/i}$ hypomorphic mice. The *Prep1*$^{i/i}$ gene was targeted in an embryonic stem cell line isolated from a library (129/SvEvBrd strain) of embryonic stem cells randomly targeted with a retroviral vector (VICTR45) at Lexicon Genetics, Inc. (The Woodlands, Texas). The details will be described elsewhere (Ferretti et al., submitted). In this paper, all *Prep1*$^{i/i}$ mice were generated by heterozygous mice backcrossed four times with wild-type C57BL/6 mice.

PCR genotyping of *Prep1*$^{i/i}$ hypomorphic mice. On the basis of the genomic sequence (19), Prep1-specific oligonucleotides Prep-F1 and Prep-R1 were synthesized. Oligonucleotide Prep-R1 was used in combination with the vector-specific LTR2 oligonucleotide to amplify 230 bp in the disrupted allele, while the combination of Prep-F1 and Prep-R1 amplifies 300 bp of the wt allele. The sequences of the oligonucleotides are as follows: Prep-F1, 5′-CCAAGGGCA GTAAGAGAAGCTCTGGAG-3′; Prep-R1, 5′-GGAGTGCCAACCATGTTA AGAAGAAGTCCC-3′; and LTR2, 5′-CAAAATGGCGTTACTTAAGCTAGC TTGCC-3′.

PCR conditions were as follows: 5 min at 95°C; 30 cycles of denaturation (45 s at 94°C), annealing (1 min at 62°C), and elongation (1 min at 72°C); followed by a final extension step (5 min at 72°C).

Antibodies. The following antibodies were used in this study: anti-CD4 (RM4-5) conjugated to CyChrome, phycoerythrin (PE), or fluorescein isothiocyanate (FITC); anti-CD8a (53-6.7) conjugated to CyChrome or allophycocyanin (APC); anti-CD3e (145-2C11) conjugated to CyChrome; anti-CD25 (7D4) conjugated to APC; anti-CD44 (IM7) conjugated to PE; anti-T-cell receptor β-chain (anti-TCRβ) (H57-597) conjugated to FITC; anti-TCRβ (H57-597) conjugated to biotin; anti-TCRγδ (GL-3); anti-CD69 (H1.2F3) conjugated to PE; anti-CD127 (SB/199) conjugated to PE; anti-CD45.1 (A20) conjugated to PE; anti-CD45.2 (104) conjugated to biotin; and anti-CD16/CD32 (Fc receptor; 24G2) (BD Biosciences, San Jose, CA).

Anti-Pbx1, anti-Pbx2, and anti-Pbx3 (SC891X) antibodies were obtained from Santa Cruz Biotechnology (Santa Cruz, CA). Anti-Prep1 (Meis4) and anti-Meis (Meis1, Meis2, and Meis3) are from Upstate Biotechnology (Upstate House, Dundee, United Kingdom). The anti-Pbx1b, anti-Pbx3a, and anti-Pbx3b antibodies were a generous gift from Michael Cleary. Anti-Prep1 polyclonal antibody was prepared in our laboratory (7).

The following secondary reagents were used: streptavidin-APC (BD Biosciences, San Jose, CA), streptavidin-FITC (Caltag Laboratories, Burlingame, CA), sheep anti-mouse and donkey anti-rabbit immunoglobulin G (IgG) labeled with horseradish peroxidase (HRP) (Amersham Biosciences, Amersham Place, United Kingdom), and rabbit anti-goat IgG labeled with horseradish peroxidase (Santa Cruz Biotechnology, Santa Cruz, CA).

Flow cytometry. Thymi, spleens, lymph nodes (LN) (inguinal, cervical, axillary, and brachial), and peripheral blood samples were obtained from littermate mice that were 6 to 12 weeks old (unless specified otherwise). Cell suspensions were obtained by gentle disruption, passage through a cell strainer (40-μm nylon), and washing the cells with phosphate-buffered saline (PBS). After red blood cell lysis, lymphocyte subsets were analyzed for detection of both surface and intracellular proteins. Briefly, 5×10^5 cells were incubated with anti-CD16/CD32 (Fc receptor) antibody to block Fc receptors. Surface staining was performed in binding buffer (PBS containing 3% fetal bovine serum [FBS] and 0.1% NaN_3) for 15 min on ice for two, three, or four colors and analyzed by a FACScan or FACSCalibur flow cytometer. For intracellular staining, cells were fixed in 2% paraformaldehyde in PBS for 10 min at room temperature and permeabilized with 0.5% saponin in PBS containing 3% FBS. Data analysis was performed with CellQuest software (BD Biosciences).

Thymocyte purification and cell sorting. Double-negative thymocytes were obtained by rabbit anti-CD4 (monoclonal antibody [MAb] 1.72) and anti-CD8 (MAb 31 M) complement-mediated lysis. Residual CD4$^+$ and CD8$^+$ cells were negatively gated by staining with CyChrome-conjugated anti-CD4 and CyChrome-conjugated anti-CD8 antibodies or further purified by magnetic beads (Miltenyi Biotec, Bergisch Gladbach, Germany) when necessary. For cell sorting, total thymocytes were stained with anti-CD4, anti-CD8, and anti-TCRβ antibodies and CD4$^+$ CD8$^+$ double-positive (DP), DN, CD4$^+$, and CD8$^+$ (CD8$^+$ αβTCR^{high} [cells with high levels of the αβT-cell receptor {αβTCR}) subpopulations of thymocytes were sorted by a FACS Vantage cell sorter.

BrdU assay. Bromodeoxyuridine (BrdU) (1 mg) was injected intraperitoneally, and the thymi were taken 1 hour after injection. Cell cycle analysis was performed with BrdU-flow kit (BD Biosciences) according to the manufacturer's recommendations.

Quantitation of apoptosis by annexin V. Thymocytes were incubated in RPMI 1640 medium containing 10% FBS, 2 mM glutamine, 25 mM HEPES, β-mercaptoethanol, and penicillin/streptomycin at a concentration of 1×10^6 cells per 200 μl in 96-well plates. Cells were collected at different time points and stained as described above with antibodies to CD4$^+$ and CD8$^+$. The percentage of annexin V-positive, 7-aminoactinomycin D (7AAD)-negative cells was determined with a FITC-annexin V kit (BD Biosciences) according to the manufacturer's recommendations.

Protein extract preparation and electrophoretic mobility shift assays. Nuclear and cytoplasmic extracts from lymphocytes were purified according to a published protocol (17). The electrophoretic mobility shift assay was performed as described previously (7). The O1 oligonucleotide probe used (5′-CACCTGAGA GTGACAGAAGGAAGGCAGGGAG-3′) contains a binding site for Prep1-Pbx from the urokinase enhancer (underlined) (7).

Immunoblotting. Nuclear and cytoplasmic protein extracts (30 μg each) were resolved by 8 to 10% sodium dodecyl sulfate-polyacrylamide gel electrophoresis and transferred to polyvinylidene difluoride (PVDF) membranes (Millipore, Billerica, MA) in a semidry blotting apparatus. The membranes were incubated with anti-Prep1 (1:2,000), anti-Pbx1b (1:1,000), anti-Pbx2 (1:2,000), and anti-Meis (1:2,000) antibodies. Blots were developed with SuperSignal Westpico or SuperSignal Westdura chemiluminescence substrate (Pierce, Rockford, IL).

Total RNA isolation and RT-PCR. RNA was isolated from thymocytes by the TRIZOL method (Invitrogen, Carlsbad, CA) according to the manufacturer's recommendations. Five million cells were used for RNA isolation from unsorted thymocytes or DP thymocytes, and 1 million cells were used for RNA isolation from DN and CD4$^+$ and CD8$^+$ SP subsets of thymocytes. RNA was reverse transcribed with SuperScript II (Invitrogen) using oligo(dT) following the instructions of the manufacturer. cDNA was amplified on a GeneAmp 2400 machine (PE Applied Biosystems, Foster City, CA) under the following conditions: 1 cycle of 94°C for 3 min; 26 cycles (for *Prep1*, *Pbx1*, and *Pbx2*) or 24 cycles (for β-*actin*), with 1 cycle consisting of 94°C for 45 s, 60°C for 1 min, and 72°C for 1

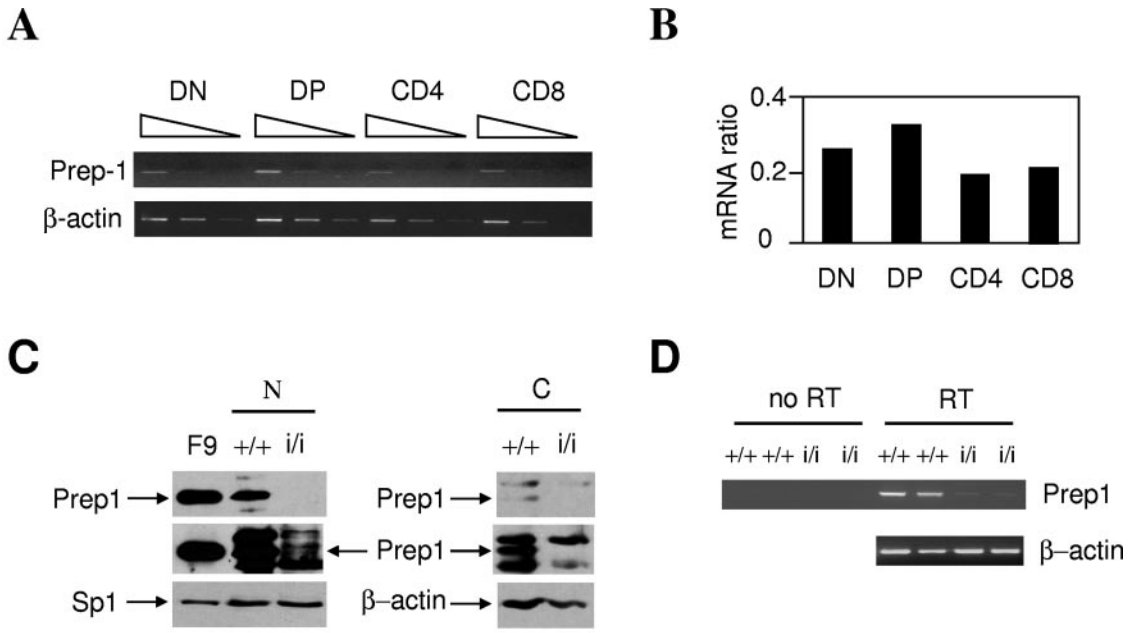

FIG. 1. Expression of Prep1 during T-cell development in wild-type and *Prep1*$^{i/i}$ mice. (A) RT-PCR analysis of sorted subpopulations of wild-type thymocytes. Total RNA was isolated from DN, DP, CD4$^+$ (CD4), and CD8$^+$ (CD8) cells. Serial dilutions (1:5) of cDNA were amplified with Prep1 and β-actin primers (see Materials and Methods). (B) Relative amounts of the Prep1 PCR product are shown in the histogram. (C) Nuclear (N) and cytoplasmic (C) extracts of *Prep1*$^{i/i}$ (i/i) and their wild-type controls (+/+) were blotted onto PVDF membranes and incubated with anti-Prep1 antibody. Nuclear extract from a Prep1-overexpressing cell line (F9) (30) was used as a positive control. Notice the overexposure of the Prep1 row (middle blot) to check for possible Prep1 protein. Anti-Sp1 and anti-β-actin antibodies were used as loading controls for nuclear and cytoplasmic extracts. (D) RT-PCR analysis of Prep1 expression. RNA was isolated from total thymocytes from two *Prep1*$^{i/i}$ mice (i/i) and their wild-type control littermates (+/+). In the case of *Prep1*$^{i/i}$ mRNA, 32 cycles of PCR were performed, while for β-actin mRNA, only 24 cycles were performed. The no-RT control shows the absence of product in a parallel reaction without the addition of reverse transcriptase. Primers for β-actin were used as a control.

min; and 1 cycle of 72°C for 5 min. *Pbx3*-specific DNA fragments (*Pbx3a* and *Pbx3b*) were amplified using the following conditions: 1 cycle of 94°C for 3 min; 28 cycles of 94°C for 45 s, 57°C for 1 min, and 72°C for 1 min; and 1 cycle of 72°C for 5 min. The following primer sets were used: for *Prep1*, 5-AGTAGGAAGCAC CAACGG-3′ and 5′-ACCTGAGCAGAAACTGGAG-3′; for *Pbx1*, 5′-CAGAGT TTGGATGAGGCGCAGG-3′ and 5′-GAACTTGCGGTGGATGATGCTG-3′; for *Pbx2*, 5′-GCCACAGCCGCACCAGCTCT-3′ and 5′-GGACACCCCACTCTC CCTG-3′; for *Pbx3*, 5′-GAGCTGGCCAAGAAATGCAG-3′ and 5′-GAAGAT GGAGTTGTTGCGTCC-3′; for β-actin, 5′-GGCATCCTGACCCTGAAGT-3 and 5′-CGGATGTCAACGTCACACTT-3. Controls without reverse transcriptase (no-RT controls) for each reverse transcriptase PCR (RT-PCR) were also performed.

In vitro proliferation of T cells. Thymocytes and lymphocytes were recovered from the thymi and lymph nodes of *Prep1*$^{i/i}$, *Prep1*$^{i/+}$, and *Prep1*$^{+/+}$ mice and labeled with (5- and 6-)carboxyfluorescein diacetate succinimidyl ester (CFSE) according to the manufacturer's instructions (Molecular Probes, Carlsbad, CA). Cells were plated on 24-well plates with different concentrations of plate-bound anti-CD3 antibody (0, 0.1, 1, and 10 μg/ml) with or without anti-CD28 antibody (5 μg/ml). The concentrations of the cells were 2×10^6 per well for thymocytes and 1×10^6 per well for lymphocytes. Three and five days later, cells were harvested, stained with anti-CD4, anti-CD8, and anti-TCRβ (in the case of thymocytes), and analyzed by flow cytometry.

Repopulation experiments. CD45.1 C57BL/6 recipient mice (6 to 8 weeks old) were lethally irradiated (1,100 cGy delivered in a single dose) using an X-ray source (150 kV, 11.9 mA). Single-cell suspensions from E14.5 wt or *Prep1*$^{i/i}$ fetal livers (FLs) were prepared by passage through a cell strainer (40-μm nylon), and two million FL CD45.2 cells from wild-type or *Prep1*$^{i/i}$ embryos were transplanted by injection into the tail veins of irradiated recipients. After FL cell transplantation, recipient mice were maintained on antibiotic water containing neomycin sulfate (0.016 g/liter). The survival of mice was monitored daily for 30 days and then once a week for 8 months after transplantation.

Apoptosis kinetic analysis. Thymocytes were incubated in RPMI 1640 medium containing 10% fetal calf serum, 2 mM glutamine, 25 mM HEPES, 100 U/ml of penicillin, and 100 U/ml of streptomycin at a concentration of 1×10^6 cells per 200 μl in 96-well plates. Cells were collected at various time points and stained as described above with anti-CD4, anti-CD8, and anti-TCRβ antibodies. The total number of viable cells was determined by trypan blue exclusion and staining of thymocytes with TOPRO-3 (Molecular Probes). The number of DN, CD4$^+$, CD8$^+$ mature, and DP thymocytes was calculated for each time point.

RESULTS

Prep1 is expressed throughout postnatal thymic development. We previously observed that *Prep1* is highly expressed in the mouse thymus (18). To better characterize *Prep1* expression during thymic development, CD4$^-$ CD8$^-$ double-negative, CD4$^+$ CD8$^+$ double-positive, CD4$^+$ CD8$^-$ and CD4$^-$ CD8$^+$ single-positive thymocytes were isolated by cell sorting and analyzed by RT-PCR. Figure 1A and B show that *Prep1* mRNA was almost uniformly expressed during thymocyte development, in keeping with a recent report (46).

To investigate the role of Prep1, we recently generated hypomorphic *Prep1*$^{i/i}$ mice (described in Materials and Methods; Ferretti et al., submitted). Embryonic fibroblasts or embryonic organs of the *Prep1*$^{i/i}$ mice contain a minor amount (5 to 10%) of the Prep1 protein, and therefore, we define *Prep1*$^{i/i}$ as an hypomorphic and not a null mutation. The *Prep1*$^{i/i}$ mutation shows an embryonic lethal phenotype with variable penetrance (after E17.5 and before P0). After four backcrosses with wild-type C57BL/6 mice, about 6% of the progeny of heterozygous crosses (instead of 25%) is constituted of homozygous *Prep1*$^{i/i}$

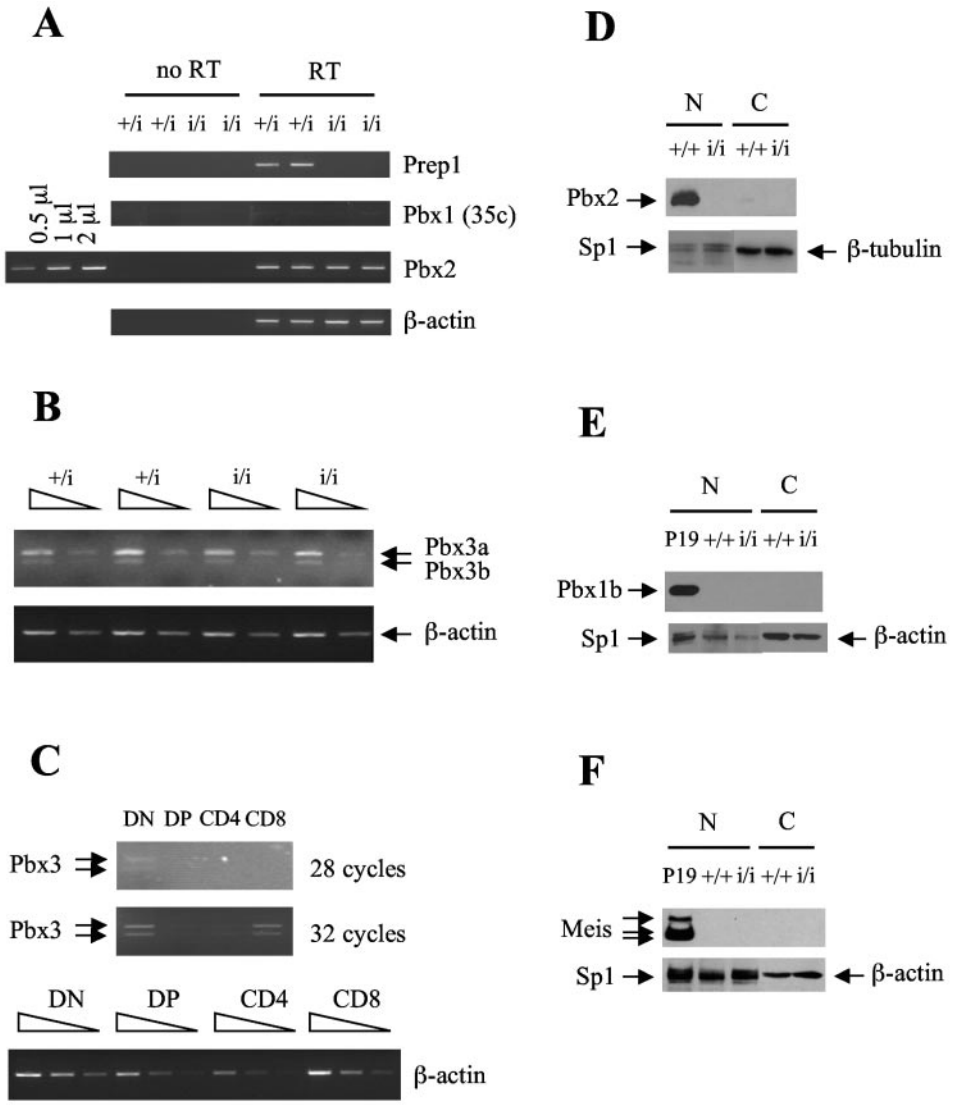

FIG. 2. Analysis of expression of Prep1, Pbx, and Meis proteins in the wild-type and *Prep1*$^{i/i}$ mice. (A) RT-PCR analysis of Prep1, Pbx1, and Pbx2 expression. RNA was isolated from thymocytes from two *Prep1*$^{i/i}$ mice (i/i) and their heterozygous *Prep1*$^{+/i}$ (+/i) control littermates. The leftmost three lanes in the third blot represent PCR (26 cycles) with increasing amounts of wild-type cDNA to determine the optimal (nonsaturating) conditions. The no-RT controls show the absence of product in parallel reactions without the addition of reverse transcriptase. PCR for Pbx1 amplification was performed for 35 cycles (35c), instead of the 26 cycles used for Prep1, β-actin, and Pbx2. Primers for β-actin were used as a control. (B) RT-PCR analysis of Pbx3 expression in total thymocytes. RNA was isolated from thymocytes from two *Prep1*$^{i/i}$ mice (i/i) and their littermate heterozygous *Prep1*$^{+/i}$ controls (+/i). Serial dilutions (1:5) of cDNA were amplified with Pbx3 and β-actin primers. PCR was performed for 28 cycles. The two PCR products correspond to Pbx3a and Pbx3b cDNA. (C) RT-PCR analysis of Pbx3 expression in subpopulations of wild-type thymocytes. RNA was isolated from DN, DP, CD4$^+$ (CD4), and CD8$^+$ (CD8) cells. cDNA was amplified with Pbx3 primers, and serial dilutions (1:5) of cDNA were amplified with β-actin primers. PCR was performed for 28 and 32 cycles (Pbx3) and for 24 cycles (β-actin). (D to F) Nuclear (N) and cytoplasmic (C) extracts of *Prep1*$^{i/i}$ (i/i) and their wild-type controls (+/+) were blotted onto PVDF membranes and incubated with anti-Pbx2 (D), anti-Pbx1b (E), or anti-Meis (F) antibodies. Anti-Sp1, anti-β-actin, and anti-β-tubulin antibodies were used as loading controls for nuclear and cytoplasmic extracts. In panels E and F, a nuclear extract of the P19 cell line induced with retinoic acid (10^{-7} M) for 24 h was used as a positive control for the expression of Pbx1b and Meis proteins.

mice which survive for at least 14 months (not shown). This frequency was not further modified in heterozygous mice backcrossed nine times with wt C57BL/6 mice (not shown). Importantly, while some *Prep1*$^{i/i}$ mice were born smaller, they recovered rapidly, and by 2 to 3 months of age, they were indistinguishable from wild-type mice. *Prep1*$^{i/i}$ mice were normally viable and fertile (data not shown).

In the thymi of *Prep1*$^{i/i}$ mice, Prep1 protein was not detectable either in the nuclear or cytoplasmic extracts (Fig. 1C). Upon overexposure of the blots, an extremely faint band comigrating with Prep1 appeared in the nuclear fraction (Fig. 1C, middle blot). Semiquantitative RT-PCR analysis of the thymi from 8-week-old mice revealed that *Prep1* mRNA was barely detectable in *Prep1*$^{i/i}$ thymus with an RT-PCR carried out for 32 cycles (Fig. 1D). This mRNA was also observed at 2 to 3% of the wt level in the E10.5

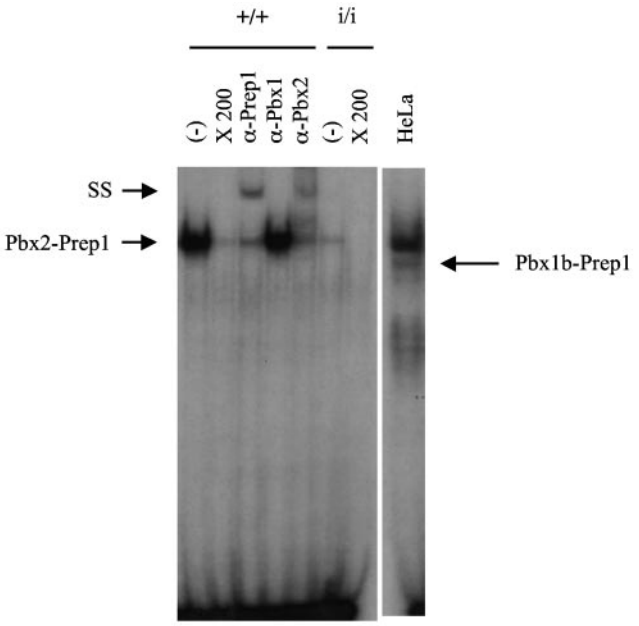

FIG. 3. Prep-Pbx DNA-binding activity of the thymus is drastically decreased in *Prep1*$^{i/i}$ thymocytes. Electrophoretic mobility shift assays were performed with the radiolabeled O1 double-stranded oligonucleotide, incubated with nuclear extracts from the thymi of wild-type (+/+) or hypomorphic *Prep1*$^{i/i}$ (i/i) mice without (−) or with the addition of 200-fold excess unlabeled O1 (X 200) or with antibodies against Prep1, Pbx1, or Pbx2 (α-Prep1, α-Pbx1, or α-Pbx2). Pbx2-Prep1 and Pbx1b-Prep1 arrows indicate the migration of complexes formed between Prep1 and Pbx2 or Prep1 and Pbx1b from HeLa cell nuclear extract. HeLa cell nuclear extract was used as a control. SS, supershift.

Prep1$^{i/i}$ whole embryo (Ferretti et al., submitted). The exact amount of *Prep1* mRNA in the thymi of *Prep1*$^{i/i}$ mice was not measured quantitatively.

The thymi from *Prep1*$^{i/i}$ mice show a major reduction of the Pbx2 level. Since no difference was observed between wt and heterozygous *Prep1*$^{+/i}$ mice (not shown), we used wt and heterozygous littermates as controls throughout the experiments reported in this paper. We showed that *Prep1* controls the level of Pbx proteins in *Prep1*$^{i/i}$ mice (Ferretti et al., submitted). We therefore analyzed the thymic expression of the TALE genes *Pbx1*, *Pbx2*, *Pbx3*, *Meis1*, *Meis2*, *Meis3*, and *Prep2*. While *Pbx1* mRNA was barely detectable, *Pbx2* and *Pbx3* (*Pbx3a* and *Pbx3b*) mRNA were expressed at visible levels in *Prep1*$^{+/i}$ mice (Fig. 2A and B). However, the level of *Pbx3* mRNA expressed was much lower (at least 10-fold) than that of *Pbx2*. Detailed RT-PCR analysis in sorted thymocyte subpopulations of wild-type C57BL/6 mice showed that *Pbx3* is expressed in DN thymocytes, down-regulated in DP thymocytes, and reexpressed again in SP (albeit, to a lesser extent) CD8$^+$ thymocytes (Fig. 2C) in agreement with a gene expression profiling study (46). The lower expression of *Pbx3* with respect to *Pbx2* can partially be explained by the fact that *Pbx3* is expressed only by some subsets of thymocytes (Fig. 2C), while Pbx2 is present at all stages of T-cell development (46).

Immunoblotting analyses of thymic extracts were next performed with antibodies specific for Pbx1b, Pbx2, and Pbx3 and with anti-Meis antibodies recognizing all three forms of Meis. We found a strong signal for Pbx2 in nuclear extracts (and no signal in cytoplasmic extracts) of *Prep1*$^{+/i}$ thymi (Fig. 2D), while no Pbx1b and none of the Meis proteins were detectable (Fig. 2E and F). Also, the Pbx3 level was below the detection limits of the antibodies (data not shown). Importantly, immunoblotting analysis of the extracts of *Prep1*$^{i/i}$ thymi showed a drastic reduction of Pbx2, which was essentially absent, in both the nucleus and cytoplasm (Fig. 2D). However, *Pbx2* mRNA (Fig. 2A) was present at the same level as in the wild-type mice, suggesting that the effect on Pbx2 protein level was posttranscriptional. No changes in the levels of *Pbx3a* and *Pbx3b* mRNA in *Prep1*$^{i/i}$ mice in comparison to wild-type (or heterozygous) mice were observed (Fig. 2B and data not shown), suggesting, but not proving, that *Pbx3* expression in thymocytes is independent of Prep1. No signal for Meis1, Meis2, Meis3, Pbx1b (or Prep2 [not shown]) was revealed in either nuclear or cytosolic extracts of *Prep1*$^{i/i}$ thymi (Fig. 2E and F; also data not shown). Therefore, the absence of Pbx2 and Prep1 is not compensated for by any of these proteins.

Finally, we performed electrophoretic mobility shift assays on nuclear extract from the thymus of a 9-week-old wild-type mouse (Fig. 3). For this assay we employed oligonucleotide O1, which has a high affinity for Prep-Pbx and Meis-Pbx dimers (9). A single band was visible; the band was displaced by an unlabeled probe and inhibited by the anti-Prep1 and anti-Pbx2 antibodies. No effect was observed with the anti-Pbx1 antibody. This result agrees with the immunoblotting results of Fig. 2 and shows that Prep1 and Pbx2 are the major DNA-binding partners and are specific for the Prep-Pbx sites. A major decrease, but not a total absence, of specific DNA-binding activity was observed with *Prep1*$^{i/i}$ thymic extracts (Fig. 3). The minor residual activity agrees with *Prep1*$^{i/i}$ mice being hypomorphic and is similar to the results obtained in whole-embryo extracts and in extracts of embryonic brain and liver (Ferretti et al., submitted).

Abnormal numbers of mature T lymphocytes are found in the peripheral lymphoid tissues and blood of *Prep1*$^{i/i}$ mice. We analyzed the composition of the different lymphoid compartments (Table 1). First, we compared the cellularity of primary and secondary lymphoid organs in 6- to 10-week-old wild-type and homozygous *Prep1*$^{i/i}$ littermates. The absolute numbers of cells in the thymi and spleens of *Prep1*$^{i/i}$ mice were indistinguishable from those of wild-type controls (Table 1) until the mice were 12 weeks old. In mice over 12 weeks of age, there was a small reduction of thymic cellularity (up to 30%), which was more evident in males, i.e., during thymic involution (Table 1). However, the absolute cell number was reduced by 50% in the lymph nodes of *Prep1*$^{i/i}$ mice compared to that in wild-type controls (Table 1).

Then we performed a flow cytometry analysis after staining of the cells with antibodies to CD4, CD8, αβTCR, and γδTCR. This analysis revealed that the percentage of CD4$^+$ or CD8$^+$ T cells was reduced by 40% in the spleen and blood and by 20 to 30% in LN derived from *Prep1*$^{i/i}$ mice compared to that in wild-type littermates (Table 1). Since the absolute number of cells was lower in the LN, the decrease in mature CD4$^+$ and CD8$^+$ cells was more than 50% (Table 1). The number of γδ T cells was increased twofold in the spleens and lymph nodes of *Prep1*$^{i/i}$ mice (not shown).

TABLE 1. T-cell populations in wild-type and *Prep1*$^{i/i}$ mice[a]

Organ	Genotype[b]	No. of cells (10^6)	No. of CD4$^+$ cells (10^6)	% CD4$^+$	No. of CD8$^+$ cells (10^6)	% CD8$^+$
Thymus (6–10w.)[c] (n = 10)	+/+	183.2 (45)	12.3 (2.9)	6.3 (0.8)	2.9 (0.9)	1.6 (0.4)
	i/i	150.4 (35)	5.1 (1.3)	3.2 (0.9)	1.1 (0.4)	0.7 (0.3)
P value[d]		NS	<0.0005	<0.0002	<0.002	<0.001
Thymus (12–16w.)[c] (n = 8)	+/+	102.1 (28)	5.5 (1.4)	5.6 (1.1)	1.3 (0.34)	1.4 (0.2)
	i/i	72.3 (26.6)	2.2 (0.6)	2.9 (0.5)	0.45 (0.25)	0.6 (0.13)
P value		<0.1	<0.001	<0.001	<0.001	<0.0002
Spleen (n = 12)	+/+	106.4 (21.7)	27.0 (5.3)	24.3 (4.2)	14.5 (3.4)	12.8 (3.3)
	i/i	120.0 (43.5)	15.1 (3.1)	13.8 (3.3)	7.9 (2.1)	7.1 (2.0)
P value		NS	<0.001	<0.0001	<0.001	<0.00005
Lymph nodes (n = 10)	+/+	23.5 (6.1)	10.1 (4.7)	45.7 (2.0)	7.1 (3.3)	31.5 (1.9)
	i/i	13.6 (5.5)	4.3 (1.7)	36.7 (3.5)	3.3 (0.4)	24.0 (2.7)
P value		<0.01	<0.0001	<0.005	<0.00002	<0.001
Blood (n = 8)	+/+	6.5 (1.1)	2.4 (0.9)	36.2 (4.1)	1.3 (0.3)	20.8 (2.1)
	i/i	6.1 (1.7)	1.4 (0.8)	22.3 (5.0)	0.9 (0.2)	13.4 (2.2)
P value		NS	NS	<0.0005	<0.05	<0.0001

[a] The data shown are mean values. Standard errors of the means are shown in parentheses. The number of cells per organ (thymus, spleen, and lymph nodes) or per milliliter of blood is shown.
[b] +/+, wild-type mice; i/i, hypomorphic *Prep1*$^{i/i}$ mice.
[c] Thymi were from 6- to 10-week-old (6–10w.) mice or 12- to 16-week-old (12–16w.) mice.
[d] The *P* values compare the values for that organ or tissue for the wild-type and *Prep1*$^{i/i}$ mice. NS, not statistically significant.

We did not study B-cell development in *Prep1*$^{i/i}$ mice, but we found no changes in the number of B lymphocytes in peripheral blood (2,700/μl ± 650/μl in wild-type mice versus 3,600/μl ± 550/μl in *Prep1*$^{i/i}$ mice) and spleen ($44.5 \times 10^6 \pm 6.3 \times 10^6$ in wild-type mice versus $43.2 \times 10^6 \pm 8.7 \times 10^6$ in *Prep1*$^{i/i}$ mice).

Analysis of T-cell development in *Prep1*$^{i/i}$ mice. Next, we studied T-cell progenitors in the thymus. Cells recovered from the thymi of 6- to 10-week-old mice were stained with anti-CD4 and anti-CD8 MAbs and analyzed by flow cytometry. Figure 4A shows one representative experiment, and Fig. 4B exhibits the data averaged from 10 mice, showing that the absolute numbers of DP thymocytes were comparable in *Prep1*$^{i/i}$ mice and control littermates. However, we found a marked (two- to threefold) decrease in CD4$^+$ and CD8$^+$ SP thymocytes (Fig. 4B and Table 1) and a clear increase in DN progenitors (Fig. 4B). DN thymocytes were analyzed by flow cytometry after staining with anti-CD25 and anti-CD44 MAbs (Fig. 4C). Both the total number of DN cells (Fig. 4B) and the numbers of DN1 (CD44$^+$ CD25$^-$), DN2 (CD44$^+$ CD25$^+$), DN3 (CD44$^-$ CD25$^+$), and DN4 (CD44$^-$ CD25$^-$) cell subpopulations were significantly increased in the thymi of *Prep1*$^{i/i}$ mice over those of wild-type littermates (Fig. 4C and D), while no difference in the frequency of the single subpopulations of DN thymocytes was observed (not shown).

Thus, suboptimal *Prep1* expression results in defective maturation of SP thymocytes, which possibly accounts for the abnormal number of mature T cells.

Pre-TCR signaling is normal in *Prep1*$^{i/i}$ mice. We then tried to understand the reasons for the increase in DN cells and decrease in SP cells in *Prep1*$^{i/i}$ mice. DN thymocyte development proceeds through the TCRβ selection dependent on the surface expression of pre-TCR (50). We reasoned that the increase in DN3 and DN4 thymocytes could be due to changes in pre-TCR expression, and we compared the levels of intracellular expression of rearranged TCR β-chain (icTCRβ) in *Prep1*$^{i/i}$ and control littermates. Twenty-five percent of DN3 thymocytes in both *Prep1*$^{i/i}$ and control mice were icTCRβ positive, while up to 80% of DN4 thymocytes expressed intracellular TCRβ (Fig. 5A and B). These results were indistinguishable from those in the literature (52) and suggested that *Prep1* deficiency did not impair intracellular pre-TCR expression. Pre-TCR signaling determines proliferation, survival, differentiation, and allelic exclusion of DN αβ thymocytes (β-selection) (49). We performed in vivo BrdU labeling experiments, which allowed us to determine the percentage of cells in the S phase of the cell cycle. The number of dividing thymocytes was not different in wild-type and *Prep1*$^{i/i}$ mice (not shown), indicating that pre-TCR signaling was not significantly altered (27).

Analysis of surface TCR expression in *Prep1*$^{i/i}$ mice. Surface αβTCR is expressed by the DP cells that have passed the positive selection and subsequently by SP CD4$^+$ and CD8$^+$ T cells. γδTCR surface expression, however, starts at the DN stage in a small subset of cells at the same time as pre-TCR expression (40). We analyzed surface αβTCR and γδTCR expression in total thymocytes. Overall, the frequency of total thymocytes expressing surface αβTCR was lower in *Prep1*$^{i/i}$ mice than the frequency in wild-type or heterozygous *Prep1*$^{i/+}$ mice (4.5% versus 10% [Fig. 5C and D; also data not shown]). Homozygous *Prep1*$^{i/i}$ DP thymocytes also showed a threefold reduction in αβTCR^{high} cells (1% versus 3%), a reduction of about 20% in αβTCR^{int} cells (cells with intracellular αβTCR expression) (36% versus 46%), and a corresponding increase in the αβTCR^{low} cell population (62% versus 51%) compared to wild-type or heterozygous *Prep1*$^{i/+}$ mice (data not shown). On the contrary, the number of γδTCR-positive cells among total thymocytes was increased in *Prep1*$^{i/i}$ mice with respect to heterozygous or wild-type mice (0.58% versus 0.22%) (Fig. 5C and D).

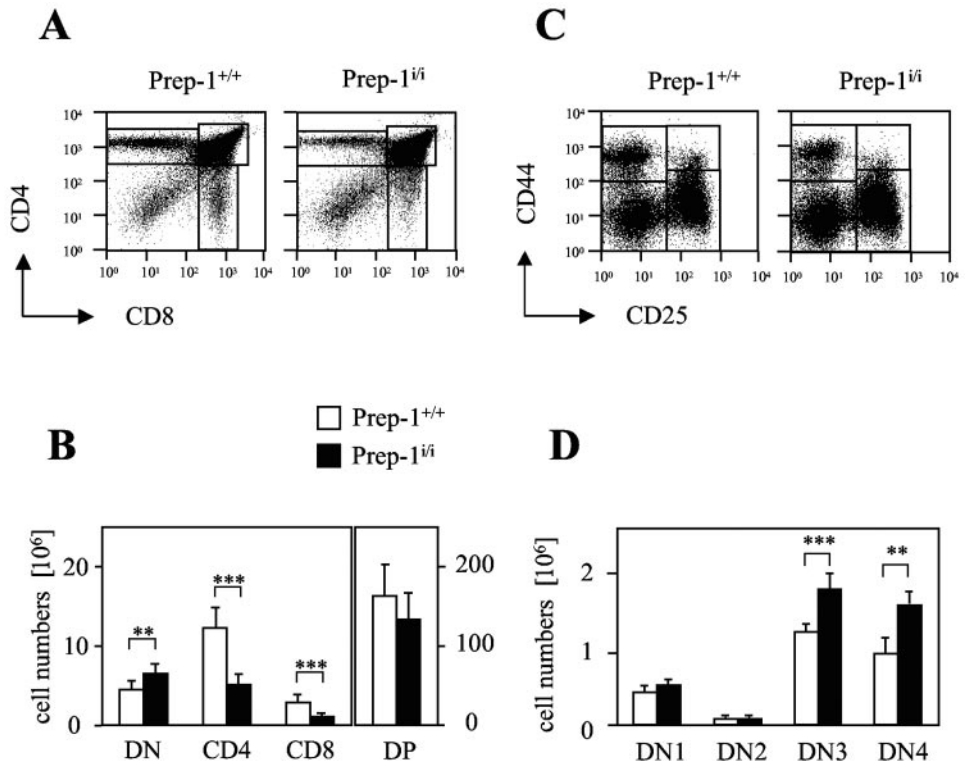

FIG. 4. Flow cytometric analysis of thymocytes from *Prep1*$^{i/i}$ mice and their wild-type controls. (A) Thymocytes were stained with PE-conjugated anti-CD4, CyChrome-conjugated anti-CD8, and FITC-conjugated anti-TCRβ antibodies. Viable cells were gated according to their forward scatter (FCS) and side scatter (SCS) characteristics. One representative of 10 independent experiments is shown. (B) Absolute numbers of DN, DP, CD4$^+$ (CD4), and CD8$^+$ (CD8) thymocytes from wild-type mice and *Prep1*$^{i/i}$ mice. Mature CD8$^+$ cells were distinguished from intermediate single-positive cells by their high αβTCR surface expression. Values that were significantly different are indicated (**, $P < 0.01$; ***, $P < 0.001$). Notice the different scale in the ordinates of DP cells. (C) Flow cytometric analysis of DN thymocytes from *Prep1*$^{i/i}$ mice and their wild-type controls. DN cells were enriched by rabbit anti-CD4 and anti-CD8 complement-mediated lysis (see Materials and Methods). DN thymocytes were stained with PE-conjugated anti-CD44 and APC-conjugated anti-CD25 antibodies. Viable cells were gated according to their FCS and SCS characteristics. One representative experiment of 10 independent experiments is shown. (D) Absolute numbers of DN1 (CD44$^+$ CD25$^-$), DN2 (CD44$^+$ CD25$^+$), DN3 (CD44$^-$ CD25$^+$), and DN4 (CD44$^-$ CD25$^-$) within DN cells. The cells were from wild-type mice (open bars) or from *Prep1*$^{i/i}$ mice (black bars). Values that were significantly different are indicated (**, $P < 0.01$; ***, $P < 0.001$).

Signaling through the TCR determines the up-regulation of CD69, a lymphocyte activation marker (22, 48), which is dependent on the protein kinase C activation pathway. In keeping with the reduced frequency of thymocytes expressing surface αβTCR, the frequency of αβTCR^{high} CD69$^+$ cells was decreased twofold in *Prep1*$^{i/i}$ mice with respect to heterozygous *Prep1*$^{i/+}$ controls when analyzed both within total thymocytes (Fig. 5E) and DP thymocyte populations (not shown). These data indicate a defect in the generation of both CD4$^+$ and CD8$^+$ SP thymocytes in *Prep1*$^{i/i}$ mice. The ratio between thymocytes expressing high and low levels of CD69 among αβTCR^{high} thymocytes was the same in control and *Prep1*$^{i/i}$ mice, showing that those cells that express CD69 contained a functional αβTCR.

The survival of DP thymocytes in *Prep1*$^{i/i}$ mice is impaired. *Prep1*$^{i/i}$ mice display a decrease in SP but not in DP thymocytes. Pro- and antiapoptotic factors are tightly regulated at this stage of development and control positive and negative selection (12, 41). We tested the tendency to apoptosis of total thymocytes by fluorescence-activated cell sorting (FACS) analysis with FITC-conjugated annexin V (see Materials and Methods). Thymocyte suspensions from *Prep1*$^{i/i}$ mice and their heterozygous control littermates were analyzed by flow cytometry measuring the percentage of 7-AAD-negative, annexin V-positive cells. The percentages of *Prep1*$^{i/i}$ DN, CD4$^+$, and CD8$^+$ cells were not different from those of controls (data not shown). However, *Prep1*$^{i/i}$ DP thymocytes displayed a higher number of 7-AAD-negative, annexin V-positive cells than control thymocytes (52% versus 37%) (Fig. 6A). This indicates that DP thymocytes from *Prep1*$^{i/i}$ mice displayed a larger frequency of apoptotic cells than their heterozygous counterpart ex vivo. The results of Fig. 6A have been reproduced with six different mice.

Even though there was a high level of apoptosis, the number of DP cells in *Prep1*$^{i/i}$ mice was not decreased (Fig. 4B). Previous reports have used in vitro culture to measure the survival capability of DP cells (32). We cultured total thymocytes for up to 60 h at 37°C. The number of viable cells was measured by flow cytometry at different intervals (see Materials and Methods). Thymocytes were stained with anti-CD4, anti-CD8, and anti-TCRβ. The absolute number of cells in each subpopulation was determined after the number of viable cells at every time point was calculated. The survival curves of DN, CD4$^+$, and CD8$^+$ cells from wild-type and *Prep1*$^{i/i}$ mice were not different (Fig. 6C and data not shown). However, as shown in

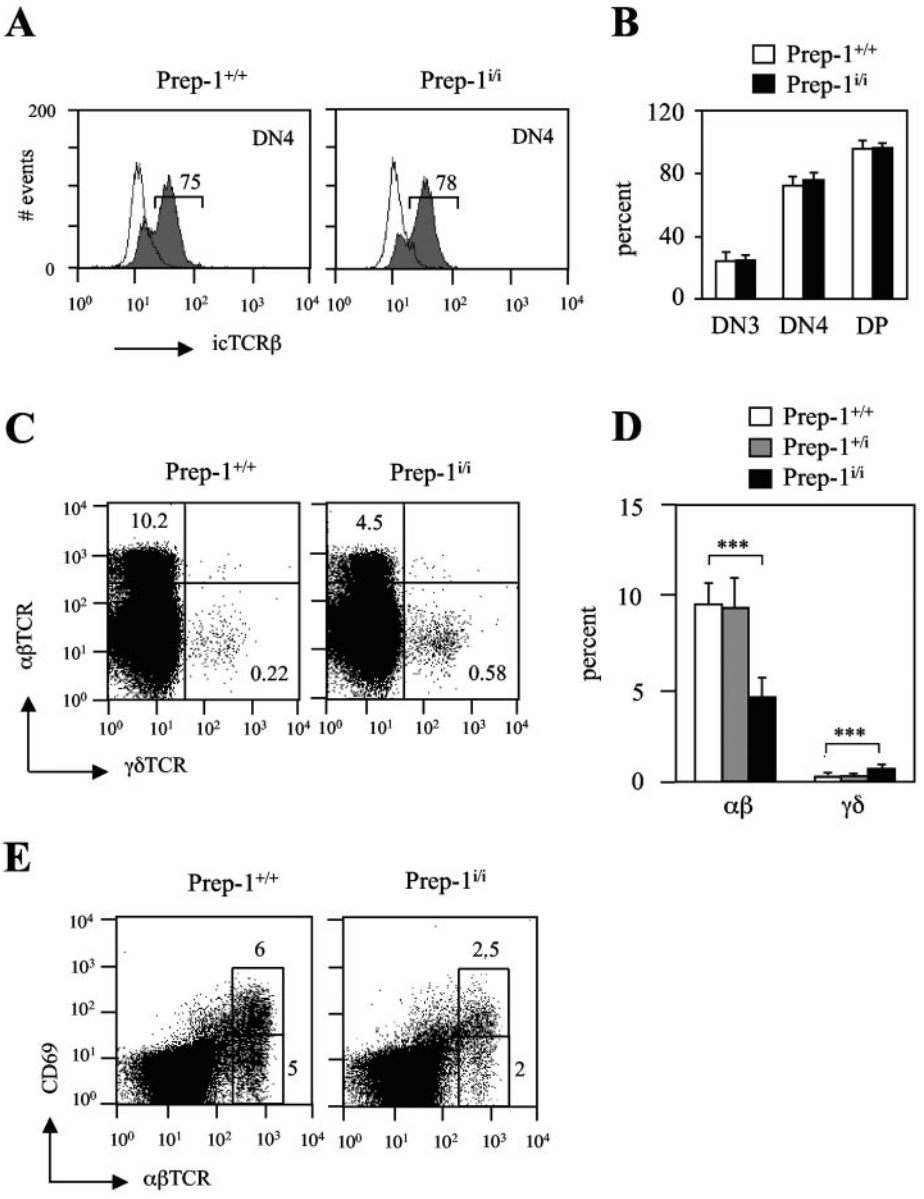

FIG. 5. Characterization of αβTCR, γδTCR, and CD69 expression in thymocytes from *Prep1*$^{i/i}$ mice. (A and B) Flow cytometric analysis of intracellular TCRβ expression in thymocytes from *Prep1*$^{i/i}$ and *Prep1*$^{+/+}$ mice. Purified DN cells were surface stained with PE-conjugated anti-CD44 and APC-conjugated anti-CD25 antibodies. DP thymocytes were directly gated after surface staining with PE-conjugated anti-CD4 and APC-conjugated anti-CD8 antibodies. Viable cells were gated according to their forward scatter (FCS) and side scatter (SCS) characteristics. Surface TCRβ was preblocked with excess unlabeled, purified MAb. Thymocytes were fixed, permeabilized, and stained intracellularly with FITC-conjugated anti-TCRβ antibody (gray histograms) or with control immunoglobulin (thin lines). (A) One example of DN4 gated thymocytes is shown. The percentage of icTCRβ-positive thymocytes is shown above the bar. (B) Average percentages of DN3, DN4, and DP thymocytes positive for icTCRβ from six *Prep1*$^{i/i}$ or wild-type control mice. (C and D) Flow cytometric analysis of surface αβTCR and γδTCR expression in total thymocytes from *Prep1*$^{i/i}$ and *Prep1*$^{+/+}$ mice. (C) Total thymocytes were stained with FITC-conjugated anti-TCRβ and APC-conjugated anti-TCRγδ antibodies. Viable cells were gated according to their FCS and SCS characteristics. The percentages of αβTCR^{high} and γδTCR^{+} cells are shown. One representative experiment of eight independent experiments is shown. (D) Average percentage of thymocytes positive for αβTCR (αβ) and γδTCR (γδ) for eight mice each for *Prep1*$^{i/i}$, heterozygous, and wild-type control mice. Values that were significantly different ($P < 0.001$) are indicated (***). (E) Total thymocytes were stained with FITC-conjugated anti-TCRβ and PE-conjugated anti-CD69 antibodies. Viable cells were gated according to their FCS and SCS characteristics. The percentages of CD69^{+}αβTCR^{high} and CD69^{+}αβTCR^{low} cells are shown in the squares. One representative experiment of eight independent experiments is shown.

Fig. 6B, the rate of disappearance of DP cells was faster in *Prep1*$^{i/i}$ mice than in the control mice. In vitro-cultured *Prep1*$^{i/i}$ DP thymocytes contained twice as many apoptotic cells (annexin V positive, 7AAD negative) even after 15 h of culture when the thymocytes triggered to die in vivo become 7AAD positive (data not shown). We conclude that ex vivo- and in vitro-cultured *Prep1*$^{i/i}$ DP thymocytes tend to have a lower survival rate or die sooner than heterozygous or wild-type

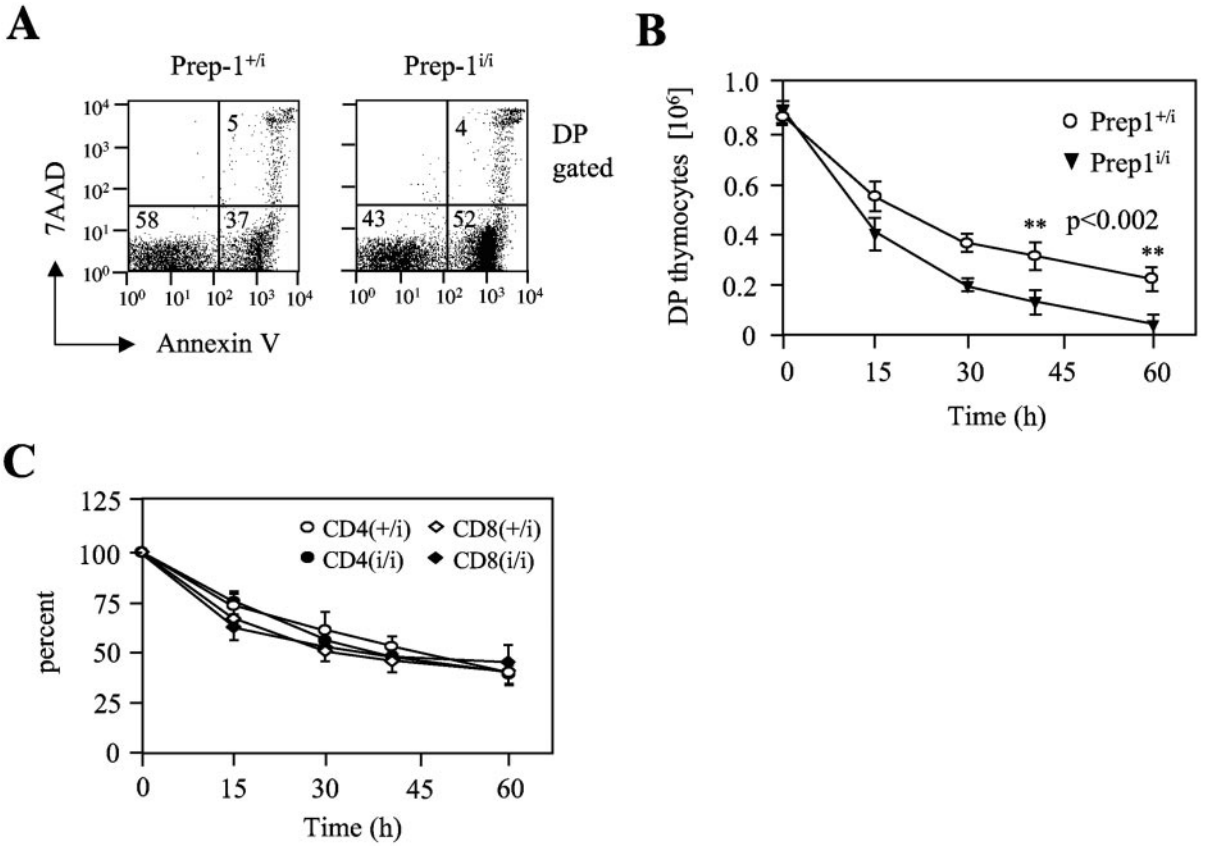

FIG. 6. Decreased in vitro survival of DP thymocytes from *Prep1*$^{i/i}$ mice. DP thymocytes from *Prep1*$^{i/i}$ mice and their heterozygous littermate controls were stained with PE-conjugated anti-CD4, APC-conjugated anti-CD8, FITC-conjugated annexin V, and 7AAD ex vivo prior to FACS analysis. (A) A representative example of DP gated thymocytes is shown. (B and C) Survival kinetics of DP (B) or of CD4$^+$ CD8$^+$ SP thymocytes (C) from *Prep1*$^{i/i}$ (i/i) mice and their heterozygous *Prep1*$^{+/i}$ (+/i) littermate controls. Thymocytes (1×10^6 cells per well in a 96-well plate) were incubated at 37°C and collected at various time points. For each time point, the total number of viable thymocytes and the percentage of DP thymocytes were determined (see Materials and Methods). In panel B, the data are expressed as the absolute number of surviving DP thymocytes; in panel C, the data are expressed as the percentage of viable CD4$^+$ CD8$^+$ thymocytes in each well.

littermate cells. This effect was specific for DP cells, and it was not noticed for any other thymocyte subpopulation.

***Prep1*$^{i/i}$ single-positive thymocytes have a lower proliferation response to stimulation with anti-CD3 or anti-CD3 plus anti-CD28.** The reduced number of SP CD4$^+$ and CD8$^+$ thymocytes as well as peripheral T cells in *Prep1*$^{i/i}$ mice can also be influenced by changes in SP thymocyte TCR-dependent proliferation (28, 29, 37). One of the well-accepted models to study TCR-induced proliferation is the CFSE dilution of CFSE-labeled cells in response to anti-CD3 stimulation (31), which can be used to mimic the activation and proliferation of lymphocytes in response to self peptide/major histocompatibility complex (MHC) (14). In order to test whether *Prep1*$^{i/i}$ cells can respond to TCR stimulation, we labeled wild-type and *Prep1*$^{i/i}$ thymocytes with CFSE and measured the in vitro proliferation capacity of SP thymocytes upon αβTCR activation with anti-CD3 alone and anti-CD3 plus anti-CD28 antibodies (see Materials and Methods). CD4$^+$ SP cells from *Prep1*$^{i/i}$ mice showed a lower proliferation capacity than CD4$^+$ SP cells from wild-type mice (most of the cells had undergone three cycles of division versus four cycles in the wild type) when stimulated with anti-CD3 and anti-CD28 antibodies. *Prep1*$^{i/i}$ CD8$^+$ SP cells showed a similar effect (four cycles versus five cycles) (Fig. 7).

The reduction of peripheral CD4$^+$ and CD8$^+$ T cells is mainly due to CD44^{low}, but not CD44^{high}, cells. *Prep1*$^{i/i}$ mice displayed a decrease in CD4$^+$ and CD8$^+$ lymphocytes in the periphery (Table 1). The number of peripheral T cells depends on thymic output, T-cell survival, and homeostatic proliferation (2, 3). In the periphery there is a pool of naïve T cells that is dependent on thymus T-cell production and a pool of activated/memory T cells capable of persisting in the absence of thymic output (47). In order to examine the activation status of peripheral *Prep1*$^{i/i}$ T cells, we investigated the relative representation of naïve (CD44^{low} [expressing low amounts of CD44]) and memory-like cells(CD44^{high}) in *Prep1*$^{i/i}$ mice in comparison with wild-type control littermates. While both the frequency (not shown) and number (Fig. 8) of CD44^{low} (naïve) cells were reduced in *Prep1*$^{i/i}$ mice for both CD4$^+$ and CD8$^+$ peripheral T cells, normal numbers of CD44^{high} CD8$^+$ T cells and only a slight reduction (30%) in CD44^{high} CD4$^+$ T cells were observed (Fig. 8). This result indicates that the reduced numbers of CD4$^+$ and CD8$^+$ T cells in the periphery may be

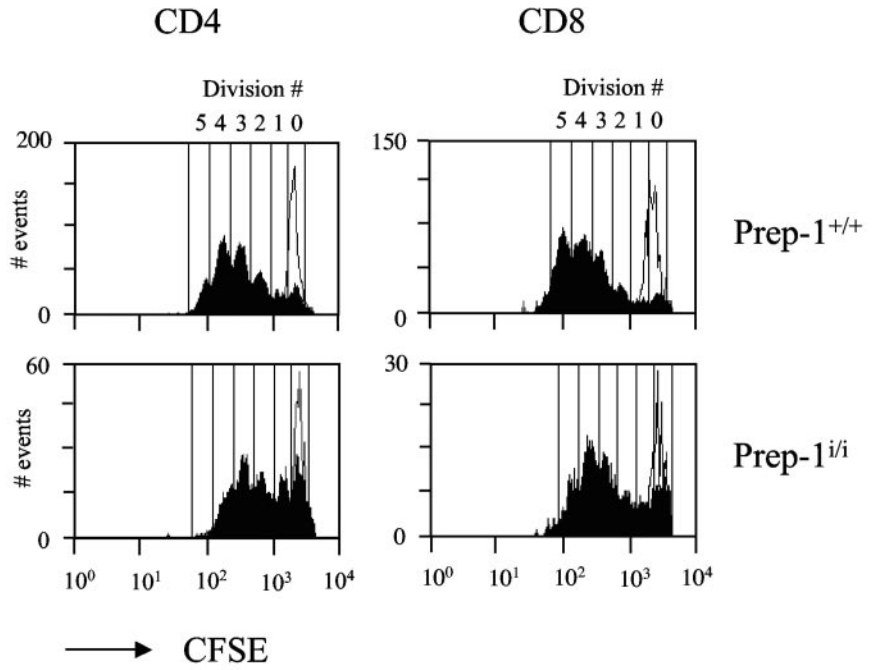

FIG. 7. In vitro proliferation of SP thymocytes after αβTCR stimulation. CFSE-labeled total thymocytes (see Materials and Methods) were stimulated by plate-bound antibodies (anti-CD3 [10 mg/ml] plus anti-CD28 [5 mg/ml]) for 3 days, stained with PE-conjugated anti-CD4 and CyChrome-conjugated anti-CD8 antibodies and analyzed by flow cytometry. CD4 and CD8 gated single-positive thymocytes from *Prep1*$^{i/i}$ mice and their wild-type littermate controls (Prep1$^{+/+}$) are shown. CFSE-labeled unstimulated cells are shown by thin lines in each histogram. The numbers of cell divisions are shown above the histograms.

due mostly to reduced thymic output and is not fully compensated by homeostatic proliferation.

The T-cell phenotype of *Prep1*$^{i/i}$ mice depends on deficiency of progenitors. Definitive hematopoiesis starts in the fetal liver around E13 to E14, from progenitors that have migrated from the aorta-gonad-mesonephros region (36). To test whether the defects in T-cell development of *Prep1*$^{i/i}$ mice were due to a deficiency in embryonic progenitors, we analyzed the repopulating activity of E14.5 fetal liver cells isolated from *Prep1*$^{i/i}$ or wild-type littermates upon transfer of the cells to lethally irradiated wild-type mice. Transplantation of two million CD45.2$^+$ *Prep1*$^{i/i}$ FL cells into lethally irradiated congenic CD45.1$^+$ wild-type mice protected against radiation death as efficiently as wild-type FL cells (data not shown). Peripheral blood samples from mice transplanted with FL cells was analyzed after 2.5 months, and the thymus and peripheral organs (blood, spleen, and lymph nodes) were recovered 8 months after transplantation. Up to 84% and 87% of peripheral blood T cells were of donor origin at 2.5 and 8 months after transplantation, respectively (not shown). At 2.5 months, *Prep1*$^{i/i}$ FL-transplanted mice showed a statistically significant decrease in both CD4$^+$ (from 14.3% ± 3.1% to 8.37% ± 3.0% [$P < 0.003$]) and CD8$^+$ (from 6.54% ± 1.6% to 2.5 ± 0.84% [$P < 0.00001$]) blood cells with respect to wild-type or heterozygous (not shown) controls. This phenotype recapitulated the one observed in *Prep1*$^{i/i}$ mice. Indeed, thymic DN cells were increased in most mice (although not to statistically significant levels), while SP CD4$^+$ and CD8$^+$ cells and αβTCR^{high} thymocytes were instead decreased (Fig. 9A). Among DN subpopulations, DN3 and DN4 subpopulations were mostly increased (not

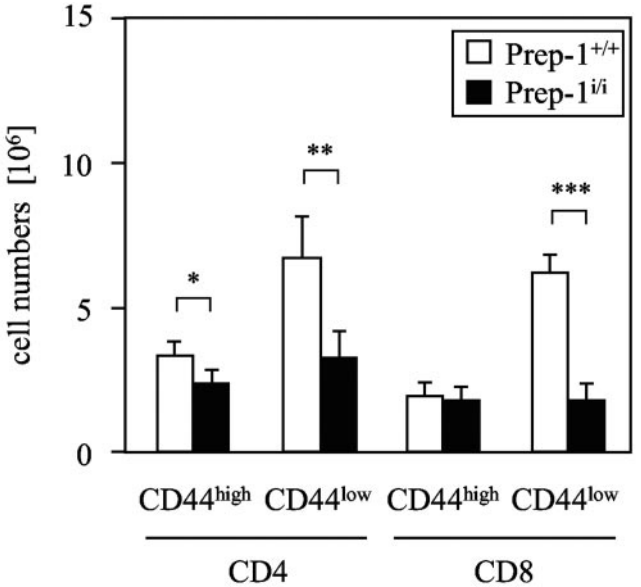

FIG. 8. The numbers of naïve CD4$^+$ and CD8$^+$ peripheral T cells were lower in *Prep1*$^{i/i}$ mice than in wild-type mice. Lymph node cells from *Prep1*$^{i/i}$ and wild-type littermates were stained with FITC-conjugated anti-CD4, APC-conjugated anti-CD8, and PE-conjugated anti-CD44 antibodies. Viable cells were gated according to their forward scatter and side scatter characteristics. The absolute numbers of CD44^{high} and CD44^{low} cells for CD4 and CD8 gated lymphocytes are shown in the histogram. Values that were significantly different are indicated (*, $P < 0.05$; **, $P < 0.01$; ***, $P < 0.001$).

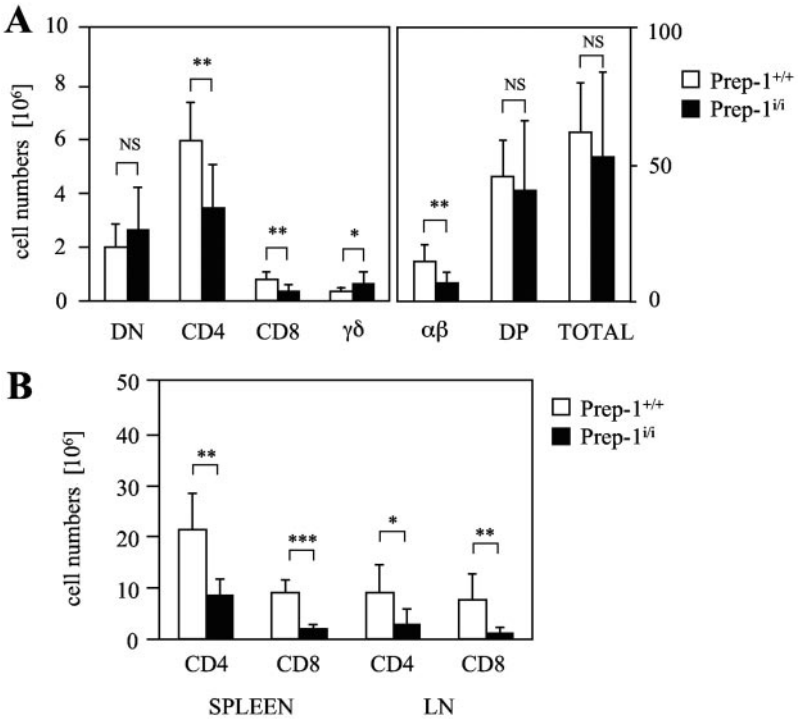

FIG. 9. Wild-type mice with E14.5 *Prep1*$^{i/i}$ FL cells transplanted recapitulate the phenotype of *Prep1*$^{i/i}$ mice. (A) Thymocyte analysis of wild-type mice transplanted with wild-type or *Prep1*$^{i/i}$ fetal liver cells. The total number of donor-derived thymocytes (gated on CD45.2-positive cells), the number of CD45.2$^+$ DN, DP, SP CD4$^+$ (CD4). and SP CD8$^+$ (CD8), αβTCR (αβ), and γδTCR (γδ) thymic cells are shown. Notice the different scale of the ordinate in the right graph. (B) Analysis of lymphocytes from the spleens and lymph nodes of mice transplanted with wild-type or *Prep1*$^{i/i}$ fetal liver cells. The absolute number of CD4$^+$ and CD8$^+$ donor-derived (gated on CD45.2-positive) T cells is shown. Values that were significantly different or not significantly different are indicated as follows: *, $P < 0.05$; **, $P < 0.01$; ***, $P < 0.001$; NS, not statistically significant.

shown). In addition, the number of γδTCR-positive cells was also doubled (Fig. 9A). In spleen and lymph nodes, again a strong reduction (three- and fivefold, respectively) was observed for CD4$^+$ and CD8$^+$ T cells in *Prep1*$^{i/i}$ FL-transplanted mice (Fig. 9B).

We conclude, therefore, that the T-cell phenotype seen in *Prep1*$^{i/i}$ mice was intrinsic to T-cell progenitors and originated from embryonic progenitors.

DISCUSSION

Prep1 and Pbx2 are involved in T-cell development. Our data establish that Prep1 and Pbx2 are the major Meinox proteins expressed in the C57BL/6 mouse thymus, with Pbx1 and Pbx3 present at extremely low levels. The analysis of hypomorphic *Prep1*$^{i/i}$ mice indicates that Prep1 and Pbx2 have important roles in T-cell development at both the postnatal and embryonic stages.

Indeed, in both the embryo and newborn mice, the most dramatic molecular phenotype of *Prep1*$^{i/i}$ mice is a drastic reduction of Pbx proteins in most organs (Ferretti et al., submitted). We have found no expression of Pbx proteins other than Pbx2 and Pbx3 (the latter at low levels and in subsets of thymocytes) (Fig. 2) in wild-type C57BL/6 mice. The Pbx2 protein was absent in *Prep1*$^{i/i}$ mice, while the level of *Pbx3* mRNA expression was not changed (Fig. 2). Moreover, the deficiency of Prep1 in *Prep1*$^{i/i}$ mice is not complemented by other Meinox family members, such as Meis1, -2, and -3 or Prep2, as they are not found in the thymi of either wild-type or *Prep1*$^{i/i}$ mice. This results in the almost complete absence of specific DNA-binding activity in the thymus extracts of *Prep1*$^{i/i}$ mice (Fig. 3). Our data agree with expression profiling studies during T-cell development, showing that *Pbx1* and *Pbx3* mRNAs, which are present in the progenitor cells (38), are turned off during thymus colonization at the DN1-DN2 transition (46). Pbx3 is then reexpressed at low levels at the DN2-DN3 transition and shut off again prior to DP formation. Pbx2, on the other hand, is expressed constitutively starting from DN1 during the entire developmental period (46).

Pbx and Meinox proteins form dimers that acquire nuclear localization and DNA-binding activity (1, 6, 9, 11). Since the major Pbx protein expressed in the thymi of wild-type mice is Pbx2, the main DNA-binding activity specific for Pbx-responsive elements depends almost exclusively on the contribution of Pbx2 and Prep1 and is almost completely absent in the *Prep1*$^{i/i}$ thymocytes (Fig. 3), especially in the DP subpopulation where *Pbx3* expression is down-regulated. In DN cells, Pbx3-Prep1 dimers might contribute to the DNA-binding activity, and the relatively mild phenotype of *Prep1*$^{i/i}$ mice at the early stages of thymocyte development might be partially accounted for by residual Pbx3-Prep1 activity present in *Prep1*$^{i/i}$ hypomorphic mice.

The decrease in Pbx2 appears to be due to a posttranscriptional mechanism (possibly protein destabilization), since the level of *Pbx2* mRNA remains normal (Fig. 2). Indeed, Prep1

appears to control both expression and stability of Pbx and Meis proteins in both mice (Ferretti et al., submitted) and zebra fish (15). A stabilizing effect of Prep1 for Pbx2 and Pbx1b was demonstrated in F9 teratocarcinoma cells overexpressing Prep1 (30).

In the thymus primordium of wild-type mice at E17.5, *Pbx2* is expressed while *Pbx1* and *Pbx3* are not. Moreover, the shorter form Pbx1b is present at low levels (44). However, while the embryos of *Pbx1*$^{-/-}$ mice (embryonic lethal at E15.5) display an ectopic thymus (43), with an anomalous formation of the third-pouch-derived thymus/parathyroid primordia, delayed expression of differentiation markers, and reduced proliferation of thymic epithelium (33), *Pbx2*$^{-/-}$ mice do not display any phenotype and are not affected in thymus development (44). However, in the *Pbx2*$^{-/-}$ mice, the absence of Pbx2 appears to be compensated for by the increase in other Pbx forms, which hence obscures the phenotype (44). The use of *Prep1*$^{i/i}$ mice has allowed us to uncover the roles of *Prep1* and *Pbx2* in thymocyte development. However, our data do not exclude an additional essential role for Pbx3.

At embryonic and postnatal stages of T-cell development, different Pbx proteins are expressed (*Pbx1* and/or *Pbx3* in the embryo versus *Pbx2* and *Pbx3* in the adult (38) (Fig. 2). Therefore, it is likely that Prep1 exhibits its functions on T-cell development by interacting with different Pbx partners at different stages. Indeed, the deficiency of *Prep1* results in reduction of Pbx proteins in both the embryo and adult (Ferretti et al., submitted).

***Prep1* deficiency hampers T-cell precursors.** The absence of Prep1 and Pbx2 in the *Prep1*$^{i/i}$ mice appears to hamper T-cell development both at the stage of embryonic progenitors and in the life of the adult. The earliest specific defect we observed in postnatal thymus was a relative 50% decrease in DN cells (Table 1 and Fig. 4). Intracellular TCRβ expression was normal in *Prep1*$^{i/i}$ mice (Fig. 5A and B), as well as the proliferation of immature T-cell precursors (data not shown). As proliferation of DN cells relies on pre-TCR expression and pre-TCR-dependent signaling (27), the normal proliferation and the absence of an anomalous frequency of single subpopulations of DN cells from *Prep1*$^{i/i}$ mice possibly indicate that pre-TCR signaling is not hampered in these cells. Indeed, there was no statistically significant reduction of DP cells in vivo, as expected. However, among DP cells, a twofold increase in apoptosis and a decrease in αβTCR^{high} thymocytes were detected (Fig. 5 and 6; also data not shown). Accordingly, we also found a twofold reduction of the CD69-expressing cells in the *Prep1*$^{i/i}$ thymus (Fig. 5E). Finally, we observed more than 50% reduction of CD4^{+} and CD8^{+} SP cells in the thymus (Table 1). γδ T cells were found to be increased by two- to threefold (Fig. 5C and D).

Prep1$^{i/i}$ embryonic progenitors of T cells were functionally impaired. Indeed, lethally irradiated mice transplanted with two million *Prep1*$^{i/i}$ FL cells developed T cells with deficiencies very similar to those of the *Prep1*$^{i/i}$ mice themselves. As shown in Fig. 9A, the thymic cellular pattern was almost identical to the pattern of *Prep1*$^{i/i}$ mice. In addition, the FL-transplanted mice displayed the same spleen and LN defects observed in the hypomorphic mice (Fig. 9B). Therefore, the defect was intrinsic to FL progenitors and did not originate in the postnatal thymus.

Functional basis of T-cell deficiency in *Prep1*$^{i/i}$ mice. Our observations indicate that Prep1 is required for T-cell development, possibly at multiple stages. The earliest defects in *Prep1*$^{i/i}$ thymocyte development were a 50% increase in DN cell number and a twofold increase in γδ T cells. This could be due to some molecular mechanisms yet to be found or simply to the reduced competition for prosurvival cytokines, such as interleukin 7 (IL-7). Indeed, IL-7 is indispensable for the normal maintenance and proliferation of both γδTCR and DN αβTCR progenitors (24, 25, 34). It was shown recently that the level of IL-7, which is produced by stromal cells, is limiting in the thymus and a down-regulation of the IL-7 receptor (IL-7R) in DP thymocytes is required in order to avoid IL-7 starvation of DN progenitors (35). IL-7R is reexpressed again during positive selection, providing necessary survival capacity to SP cells by up-regulating Bcl-2 (35). In *Prep1*$^{i/i}$ mice there was a two- to threefold reduction of αβTCR^{high} cells (Fig. 5) and a corresponding decrease in IL-7R-positive thymocytes, as confirmed by both RT-PCR and FACS analysis (data not shown). As a consequence, more IL-7 might be available to DN and γδTCR progenitors.

In *Prep1*$^{i/i}$ mice there was a twofold reduction of the total αβTCR^{high} thymocytes. The number of αβTCR^{high} CD69^{+} thymocytes was also reduced, and the same decrease was already seen among DP thymocyte subpopulations. CD69 is a marker of positive selection and is transiently up-regulated on the αβTCR^{int} and αβTCR^{high} thymocytes developing in the presence of selecting ligand/MHC (45). In contrast, DP thymocytes developing in the absence of selecting MHC complexes could not be induced to up-regulate CD69 by TCR cross-linking even when they express high-density αβTCR (45). In *Prep1*$^{i/i}$ mice, apart from the αβTCR^{high} cell reduction, there was also a 20% decrease in αβTCR^{int} cells among DP thymocytes, indicating that a loss of Prep1 blocks the early DP conversion from TCR^{low} to CD4^{low} CD8$^{low/+}$ TCR^{int} stage. The failure of DP thymocytes to mature to TCR^{int} and TCR^{high} stages might account for the increased frequency of apoptotic cells, possibly dying by neglect. Indeed, we showed that in vitro survival of DP thymocytes was impaired and the percentage of apoptotic cells increased. One of the critical players in DP thymocyte survival, Bcl-xL, is important for DP survival prior to selection signals (12, 41). We checked the expression of Bcl-xL protein by Western blotting analysis and found that it was normal in *Prep1*$^{i/i}$ thymocytes (data not shown). Thus, BcL-xL dysregulation does not appear to account for the increased frequency of apoptotic cells in *Prep1*$^{i/i}$ mice.

The reduced survival of DP thymocytes could at least in part account for the reduced number of SP cells. However, we also found that SP thymocytes from *Prep1*$^{i/i}$ mice proliferated less to TCR stimulation in vitro (Fig. 7). The proliferation rate of SP thymocytes in wild-type mice greatly influences the number of mature T cells leaving the thymus, since around 50% of them have divided in the last 24 h of their development in the thymus. Calculations show that the thymic production is roughly doubled due to this late thymocyte expansion (29). Therefore, the reduced proliferative ability of SP cells might account for the decreased number of peripheral lymphocytes.

The *Prep1*$^{i/i}$ mutation affected not only thymic, but also peripheral T cells. A twofold decrease in CD4^{+} and CD8^{+} lymphocytes was also present in the periphery, i.e., spleen, blood,

and LN (Table 1). The total number of B cells was not changed (data not shown). Spleen cellularity was normal in the tested *Prep1*$^{i/i}$ mice, possibly because the decrease in lymphocyte number was compensated for by an increase in Ter-119-positive erythroid progenitors (data not shown). The LNs from *Prep1*$^{i/i}$ mice were smaller and contained 30 to 50% fewer cells.

The decrease in CD4$^+$ and CD8$^+$ T cells in the periphery was mainly accounted for by the reduction of the naïve (CD44^{low}) cells, while the number of memory (or memory-like) CD44^{high} cells remained normal (CD8$^+$) or was reduced only 30% (CD4$^+$). The almost normal number of CD44^{high} cells could be explained by the fact that peripheral T cells might be undergoing lymphopenia-driven homeostatic proliferation and acquire a memory-like phenotype. This is usually more pronounced in CD8$^+$ cells than in CD4$^+$ T cells, thus explaining the difference between CD4$^+$ and CD8$^+$ lymphocytes (5, 13). In spite of possible homeostatic compensatory mechanisms, the naïve T-cell pool (CD44^{low}) is mostly dependent on thymus T-cell production to reconstitute the peripheral space (3, 20). We are currently dissecting the relative contribution of homeostatic proliferation versus thymic output to better understand the peripheral phenotype of *Prep1*$^{i/i}$ mice.

In conclusion, our data show that *Prep1*, *Pbx2*, and possibly Pbx3 are required for correct T-cell development. The fact that the defect in T-cell development in *Prep1*$^{i/i}$ mice is only partial (i.e., a decrease of 50 to 75% in peripheral mature T cells) is most likely due to the hypomorphic nature of the *Prep1* mutation and suggests that a complete lack of the protein would result in a more severe T-cell phenotype (possibly ablation). However, conditional knockout mice will be required to prove this point.

ACKNOWLEDGMENTS

This work was supported by grants from Telethon Fondazione Onlus, the Italian Ministry for Education and Research (MIUR), and the Italian Association for Cancer Research (AIRC). Dmitri Penkov is grateful to the Federation of European Biochemical Societies (FEBS) and to EMBO (European Molecular Biology Organization) for fellowships.

We are very grateful to M. Cleary who provided us with anti-Pbx1b, anti-Pbx3a, and anti-Pbx3b monoclonal antibodies.

REFERENCES

1. **Abu-Shaar, M., H. D. Ryoo, and R. S. Mann.** 1999. Control of the nuclear localization of Extradenticle by competing nuclear import and export signals. Genes Dev. **13:**935–945.
2. **Allen, J. M., K. A. Forbush, and R. M. Perlmutter.** 1992. Functional dissection of the *lck* proximal promoter. Mol. Cell. Biol. **12:**2758–2765.
3. **Almeida, A., J. A. Borghans, and A. A. Freitas.** 2001. T cell homeostasis: thymus regeneration and peripheral T cell restoration in mice with a reduced fraction of competent precursors. J. Exp. Med. **194:**591–599.
4. **Azcoitia, V., M. Aracil, A. Carlos-Martinez, and M. Torres.** 2005. The homeodomain protein Meis1 is essential for definitive hematopoiesis and vascular patterning in the mouse embryo. Dev. Biol. **280:**307–320.
5. **Bender, J., T. Mitchell, J. Kappler, and P. Marrack.** 1999. CD4$^+$ T cell division in irradiated mice requires peptides distinct from those responsible for thymic selection. J. Exp. Med. **190:**367–374.
6. **Berthelsen, J., C. Kilstrup-Nielsen, F. Blasi, F. Mavilio, and V. Zappavigna.** 1999. The subcellular localization of PBX1 and EXD proteins depends on nuclear import and export signals and is modulated by association with PREP1 and HTH. Genes Dev. **13:**946–953.
7. **Berthelsen, J., J. Vandekerkhove, and F. Blasi.** 1996. Purification and characterization of UEF3, a novel factor involved in the regulation of the urokinase and other AP-1 controlled promoters. J. Biol. Chem. **271:**3822–3830.
8. **Berthelsen, J., V. Zappavigna, E. Ferretti, F. Mavilio, and F. Blasi.** 1998. Prep1, a novel partner of Pbx proteins, modifies Pbx-Hox protein cooperativity. EMBO J. **17:**1434–1445.
9. **Berthelsen, J., V. Zappavigna, F. Mavilio, and F. Blasi.** 1998. Prep1, a novel functional partner of Pbx proteins. EMBO J. **17:**1423–1433.
10. **Burglin, T.** 1997. Analysis of TALE superclass homeobox genes (MEIS, PBC, KNOX, Iroquois, TGIF) reveals a novel domain conserved between plants and animals. Nucleic Acids Res. **25:**4173–4180.
11. **Chang, C. P., Y. Jacobs, T. Nakamura, N. Jenkins, N. G. Copeland, and M. L. Cleary.** 1997. Meis proteins are major in vivo DNA binding partners for wild-type but not chimeric Pbx proteins. Mol. Cell. Biol. **17:**5679–5687.
12. **Chao, D., and S. Korsmeyer.** 1998. BCL-2 family: regulators of cell death. Annu. Rev. Immunol. **16:**395–419.
13. **Dai, Z., and F. G. Lakkis.** 2001. Secondary lymphoid organs are essential for maintaining the CD4, but not CD8, naive T cell pool. J. Immunol. **167:**6711–6715.
14. **Davey, G., S. L. Schober, B. T. Endrizzi, A. K. Dutcher, S. J. Jameson, and K. A. Hogquist.** 1998. Preselection thymocytes are more sensitive to T cell receptor stimulation than mature T cells. J. Exp. Med. **188:**1867–1874.
15. **De Florian, G., N. Tiso, E. Ferretti, F. Blasi, M. Bortolussi, and F. Argenton.** 2004. Prep1.1 has essential and unique genetic functions in hindbrain development and neural crest cell differentiation. Development **131:**613–627.
16. **Dimartino, J., L. Selleri, D. Traver, M. Firpo, J. Rhee, R. Warnke, S. O'Gorman, I. L. Weissman, and M. L. Cleary.** 2001. The Hox cofactor and proto-oncogene Pbx1 is required for maintenance of definitive hematopoiesis in the fetal liver. Blood **98:**618–626.
17. **Dyer, R. B., and N. K. Herzog.** 1995. Isolation of intact nuclei for nuclear extract preparation from a fragile B-lymphocyte cell line. BioTechniques **19:**192–195.
18. **Ferretti, E., H. Schulz, D. Talarico, F. Blasi, and J. Berthelsen.** 1999. The Pbx-regulating protein Prep-1 is present in a Pbx-complexed form throughout mouse embryogenesis. Mech. Dev. **83:**53–64.
19. **Fognani, C., C. Kilstrup-Jensen, E. Ferretti, V. Zappavigna, and F. Blasi.** 2002. Human PREP-2, a novel interactor of PBX proto-oncogene, defines a novel subfamily of TALE homeodomain transcription factors. Nucleic Acids Res. **30:**2043–2051.
20. **Ge, Q., H. Hu, H. N. Eisen, and J. Chen.** 2002. Different contributions of thymopoiesis and homeostasis-driven proliferation to the reconstitution of naive and memory T cell compartments. Proc. Natl. Acad. Sci. USA **99:**2989–2994.
21. **Haller, K., I. Rambaldi, E. Nagy Kovacs, E. Daniels, and M. S. Featherstone.** 2002. Prep2: cloning and expression of a new Prep family member. Dev. Dyn. **225:**358–364.
22. **Hara, T., L. K. Jung, J. M. Bjorndahl, and S. M. Fu.** 1986. Human T cell activation. III. Rapid induction of a phosphorylated 28 kD/32 kD disulfide-linked early activation antigen (EA 1) by 12-O-tetradecanoyl phorbol-13-acetate, mitogens, and antigens. J. Exp. Med. **164:**1988–2005.
23. **Hisa, T., S. E. Spence, R. A. Rachel, M. Fujita, T. Nakamura, J. M. Ward, D. E. Devor-Henneman, Y. Saiki, H. Kutsuna, L. Tessarollo, N. A. Jenkins, and N. G. Copeland.** 2004. Hematopoietic, angiogenic and eye defects in Meis1 mutant animals. EMBO J. **23:**450–459.
24. **Kang, J., M. Coles, and D. H. Raulet.** 1999. Defective development of gamma-delta T cells in interleukin 7 receptor-deficient mice is due to impaired expression of T cell receptor genes. J. Exp. Med. **190:**973–982.
25. **Kang, J., A. Volkmann, and D. H. Raulet.** 2001. Evidence that gamma-delta versus alpha-beta T cell fate determination is initiated independently of T cell receptor signaling. J. Exp. Med. **193:**689–698.
26. **Kim, S. K., L. Selleri, J. S. Lee, Y. Jacobs, and M. L. Cleary.** 2002. Defective pancreas development and function in mice deficient for Pbx1. Nat. Genet. **30:**430–435.
27. **Kruisbeek, A., M. C. Haks, M. Carleton, A. M. Michie, J. C. Zuniga-Pflucker, and D. L. Wiest.** 2000. Branching out to gain control: how the pre-TCR is linked to multiple functions. Immunol. Today **21:**637–644.
28. **Le Campion, A., B. Lucas, N. Dautigny, S. Leaument, F. Vasseur, and C. Penit.** 2002. Quantitative and qualitative adjustment of thymic T cell production by clonal expansion of premigrant thymocytes. J. Immunol. **168:**1664–1671.
29. **Le Campion, A., F. Vasseur, and C. Penit.** 2000. Regulation and kinetics of premigrant thymocyte expansion. Eur. J. Immunol. **30:**738–746.
30. **Longobardi, E., and F. Blasi.** 2003. Overexpression of PREP-1 leads to a functionally relevant increase of PBX-2 by preventing its degradation. J. Biol. Chem. **278:**39235–39241.
31. **Lyons, A., and C. R. Parish.** 1994. Determination of lymphocyte division by flow cytometry. J. Immunol. Methods **171:**131–137.
32. **Ma, A., J. C. Pena, B. Chang, E. Margosian, L. Davidson, F. W. Alt, and C. B. Thompson.** 1995. Bclx regulates the survival of double positive thymocytes. Proc. Natl. Acad. Sci. USA **92:**4763–4767.
33. **Manley, N., L. Selleri, A. Brendolan, J. Gordon, and M. L. Cleary.** 2004. Abnormalities of caudal pharyngeal pouch development in Pbx1 knockout mice mimic loss of Hox3 paralogs. Dev. Biol. **276:**301–312.
34. **Moore, T., U. von Freeden-Jeffry, R. Murray, and A. Zlotnik.** 1996. Inhibition of gamma delta T cell development and early thymocyte maturation in IL-7−/− mice. J. Immunol. **157:**2366–2373.
35. **Munitic, I., J. A. Williams, Y. Yang, B. Dong, P. J. Lucas, N. El Kassar, R. E. Gress, and J. D. Ashwell.** 2004. Dynamic regulation of IL7-receptor expression is required for normal thymopoiesis. Blood **104:**4165–4172.

36. **Orkin, S. H.** 2000. Diversification of haematopoietic stem cells to specific lineages. Nat. Rev. Genet. **1:**57–64.
37. **Penit, C., and F. Vasseur.** 1997. Expansion of mature thymocyte subsets before emigration to the periphery. J. Immunol. **159:**4848–4856.
38. **Pineault, N., C. D. Helgason, J. H. Lawrence, and K. R. Humphries.** 2002. Differential expression of Hox, Meis1 and Pbx1 genes in primitive cells throughout murine hematopoietic ontogeny. Exp. Hematol. **30:**49–57.
39. **Rhee, J. W., A. Arata, L. Selleri, Y. Jacobs, S. Arata, H. Onimaru, and M. L. Cleary.** 2004. Pbx3 deficiency results in central hypoventilation. Am. J. Pathol. **165:**1343–1350.
40. **Saint-Ruf, C., M. Panigada, O. Azogui, P. Debey, H. von Boehmer, and F. Grassi.** 2000. Different initiation of pre-TCR and γδTCR signalling. Nature **406:**524–527.
41. **Schmitz, I., L. K. Clayton, and E. L. Reinherz.** 2003. Gene expression analysis of thymocyte selection in vivo. Int. Immunol. **15:**1237–1248.
42. **Schnabel, C., L. Selleri, Y. Jacobs, R. Warnke, and M. L. Cleary.** 2001. Expression of Pbx1b during mammalian organogenesis. Mech. Dev. **100:**131–135.
43. **Selleri, L., M. J. Depew, Y. Jacobs, S. K. Chanda, K. Y. Tsang, K. S. E. Cheah, J. L. R. Rubenstein, S. O'Gorman, and M. L. Cleary.** 2001. Requirement for Pbx1 in skeletal patterning and programming chondrocyte proliferation and differentiation. Development **128:**3543–3557.
44. **Selleri, L., J. DiMartino, J. van Deursen, A. Brendolan, M. Sanyal, E. Boon, T. Capellini, K. S. Smith, J. Rhee, H. Popperl, G. Grosveld, and M. L. Cleary.** 2004. The TALE homeodomain protein Pbx2 is not essential for development and long-term survival. Mol. Cell. Biol. **24:**5324–5331.
45. **Swat, W., M. Dessing, H. von Boehmer, and P. Kisielow.** 1993. CD69 expression during selection and maturation of CD4+8+ thymocytes. Eur. J. Immunol. **23:**739–746.
46. **Tabrizifard, S., A. Olaru, J. Plotkin, M. Fallahi-Sichani, F. Livak, and H. H. Petrie.** 2004. Analysis of transcription factor expression during discrete stages of postnatal thymocyte differentiation. J. Immunol. **173:**1094–1102.
47. **Tanchot, C., and B. Rocha.** 1998. The organization of mature T-cell pools. Immunol. Today **19:**575–579.
48. **Testi, R., J. H. Phillips, and L. L. Lanier.** 1989. T cell activation via Leu-23 (CD69). J. Immunol. **143:**1123–1128.
49. **Vasseur, F., A. Le Campion, and C. S. Penit.** 2001. Scheduled kinetics of cell proliferation and phenotypic changes during immature thymocyte generation. Eur. J. Immunol. **31:**3038–3047.
50. **Von Boehmer, H., and H. J. Fehling.** 1997. Structure and function of the pre-TCR cell receptor. Annu. Rev. Immunol. **15:**433–452.
51. **Waskiewicz, A. J., H. A. Rikhof, R. E. Hernandez, and C. B. Moens.** 2001. Zebrafish Meis functions to stabilize Pbx proteins and regulate hindbrain patterning. Development **128:**4139–4151.
52. **Wilson, M. A., M. Capone, and H. R. McDonald.** 1999. Unexpectedly late expression of intracellular CD3epsilon and TCR gammadelta proteins during adult thymus development. Int. Immunol. **11:**1642–1650.